**DE GRUYTER** OPEN Open Phys. 2015; 13:72-77

**Research Article Open Access** 

Joanna Rymarczyk\*, Lukasz Kolodziejczyk, and Elzbieta Czerwosz

# Topography, mechanical and tribological properties of nanocomposite carbon-palladium films

Abstract: In this work, the differences in nanomechanical properties, topography and morphology of carbonpalladium (C-Pd) films were studied. These films were prepared with a Physical Vapour Deposition method on various substrates with different technological parameters. We show that duration of the PVD process is a crucial factor affecting the palladium content in these films. The differences in thickness of films depend on the distance between source boats and substrates. The nanomechanical properties of C-Pd films were studied with nanoindentation. Their topography and morphology was ascertained with Atomic Force Microscopy and Scanning Electron Microscopy. It was found that the mechanical properties of C-Pd films depend on the content of palladium and on the morphology and topography of these films. The various types of carbon-palladium films containing palladium nanograins incorporated in a carbon matrix that were, investigated in this paper, seem to be promising materials for numerous applications.

**Keywords:** carbon; palladium; hardness; elastic modulus; nanoscratch

**PACS:** 68.35.Gy, 81.05.-t, 81.07.-b, 81.65.-b

DOI 10.1515/phys-2015-0004 Received January 27, 2014; accepted August 19, 2014

Lukasz Kolodziejczyk: Institute of Materials Science and Engineering, Lodz University of Technology, Stefanowskiego 1/15, 90-924 Lodz, Poland

11, 03-450 Warsaw, Poland

## Elzbieta Czerwosz: Tele and Radio Research Institute, Ratuszowa

#### 1 Introduction

Nanostructural carbonaceous films containing palladium nanograins (C-Pd films) are new nanocomposite materials with unique properties and structure in comparison with both bulk Pd and carbonaceous macro-materials [1– 4]. These materials can be used in hydrogen/hydrogen compounds sensing applications [5, 6], and thus identifying their mechanical properties such as nanohardness, reduced modulus of elasticity or delamination is particularly interesting. These properties allow the behaviour of C-Pd films to be predicted in an atmosphere containing gas with hydrogen or hydrogen compounds, at different pressure and temperature values. Even a small change in the composition or form of nanomaterials, for instance in the size and shape of Pd nanograins, as well as the type of carbonaceous matrix, affects their hydrogen sensing response. This nanomaterial is characterised by a large surface to volume ratio, therefore the superficial and near surface properties have a huge impact on understanding the mechanisms of interaction of H<sub>2</sub>-(C-Pd) films. Quantitative assessment of the mechanical properties of thin films is important to guarantee the reliability not only of the thin film but also of the mechanical detector system. The adhesion between the thin film and the substrate significantly influences the durability of the thin film [7]. We present the results of studies of carbon-palladium films obtained on various substrates using physical vapour deposition process (PVD) with different technological parameters. The nanomechanical properties of such films were examined with a nanoindentation method, a technique designed to measure the mechanical properties of materials in the nanoscale [8, 9]. We found that the mechanical properties of C-Pd films depend on the content of palladium as well as on the structure and topography of carbonaceous matrix.

<sup>\*</sup>Corresponding Author: Joanna Rymarczyk: Tele and Radio Research Institute, Ratuszowa 11, 03-450 Warsaw, Poland, E-mail: joanna.rvmarczyk@itr.org.pl

### 2 Experiment

C-Pd films were obtained by use of the PVD method with  $C_{60}$  fullerenes and palladium acetate serving as precursors. Both compounds were evaporated from two separated sources in a dynamic  $10^{-3}$  Pa vacuum [10, 11]. C-Pd films were deposited onto an Si substrate with diamond-like carbon (DLC) or  $SiO_2$  layers to separate the C-Pd films from the conductive substrate and to improve the adhesion of the C-Pd film to the substrate. DLC layer was deposited onto the Si substrate by radio frequency plasma assisted chemical vapor deposition method (RF PACVD). Silicon dioxide layer was obtained by the thermal oxidation of silicon at a temperature of  $1000^{\circ}$ C in the presence of water vapor with an oxygen flow rate of 1 L/min in time of 50 minutes. Table 1 presents the parameters of the PVD process.

Table 1: Technological parameters of PVD processes.

$I_{C60}$ [A]	$I_{Pd}$ [A]	t [min]	d [mm]	Substrate
2.1	1.2	10	69	DLC/Si
2.1	1.2	10	54	SiO <sub>2</sub> /Si
2.1	1.1	8	69	SiO <sub>2</sub> /Si
	2.1	2.1 1.2 2.1 1.2	2.1 1.2 10 2.1 1.2 10	2.1 1.2 10 69 2.1 1.2 10 54

Depending on technological parameters of the PVD process, such as current intensity through sources ( $I_{C60}$ ,  $I_{Pd}$ ), source-substrate distance (d) or deposition time (t), C-Pd films with various thickness, structure, morphology, topography and Pd content were obtained. The topography and average roughness (Ra) of these films was analysed with an atomic force microscope (model AFM - EX-PLORER 2000) in a non-contact mode, with a standard Si<sub>3</sub>N<sub>4</sub> cantilever (model MLCT-EXMT-A) in the ambient atmosphere. Grain size studies were performed with a crosssection analysis tool. The average roughness is an arithmetic mean of the absolute values of the measured profile height deviation. Additionally, the topography of C-Pd films was analysed with a scanning electron microscope (SEM), (model JEOL-JSM 7600F) operating at an incident energy of 5 keV. Pd concentration in all films was studied with the use of an Energy Dispersive X-ray Spectroscopy (EDS) technique. The surface mechanical properties of thin films were investigated with an Agilent Nano Indenter (model G200). All experiments were performed with a diamond Berkovich tip. The continuous stiffness measurement (CSM) method [12] was used to study the contact stiffness, elastic modulus and hardness of C-Pd films. Additionally, delamination of C-Pd films was investigated by a scratch test using a nanoindenter equipped with diamond conical tip of radius of 1  $\mu m$  and an apex angle of  $90^{\circ}$ .

#### 3 AFM and SEM results

All C-Pd films obtained with the PVD method have a different topography. On the surface of P1 (Figure 1) carbonpalladium nanograins are observed. The average roughness of P1 is 4.65 nm. On the surface, one can see two kinds of grains: smaller ones with a diameter ranging from 10 to 20 nm and larger ones with a diameter of  $\sim$ 100 nm. These grains have different shapes and sharp edges. AFM and SEM images of sample P2 (Figure 2) show that this film is composed of smaller grains than P1. From the analysis of the AFM image it is seen that individual grains have an oval shape and cover the entire surface. The height of the grains is 10 nm. The average roughness of P2 is similar to sample P1 at 4.7 nm. The surface of P3 differs significantly from the previous samples. It can be seen that on the surface there are no clearly visible large carbonpalladium grains, the surface is very smooth and it looks uniform. The AFM and SEM images of P3 are presented in Figure 3. The average roughness for this sample is the lowest at 1.34 nm.

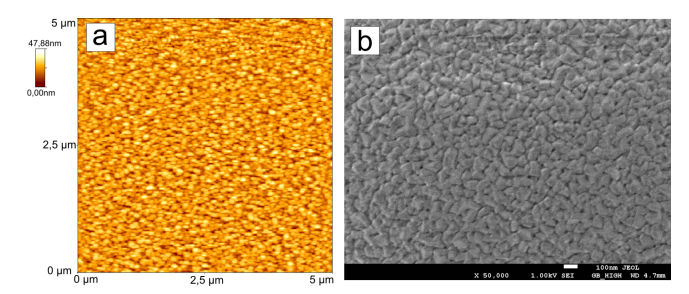


Figure 1: AFM (5  $\mu$ m × 5  $\mu$ m) and SEM images of P1.

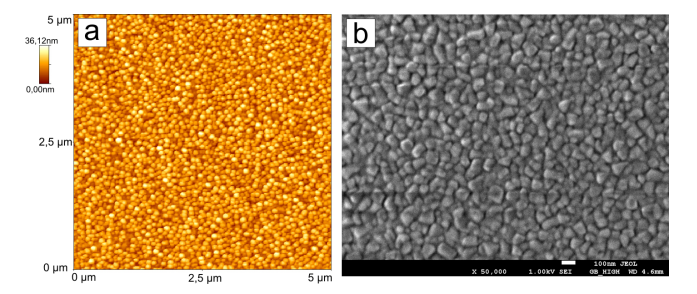


Figure 2: AFM (5  $\mu$ m × 5  $\mu$ m) and SEM images of P2.

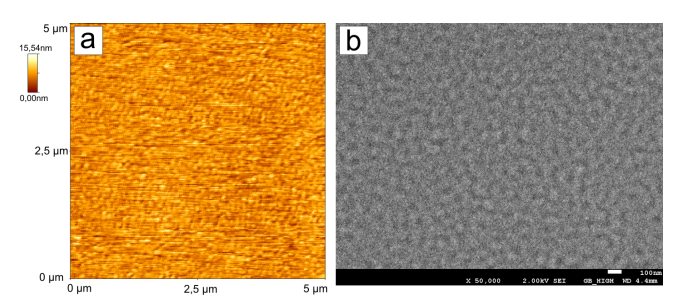


Figure 3: AFM (5  $\mu$ m × 5  $\mu$ m) and SEM images of P3.

The method of Energy Dispersive Spectroscopy (EDS) was used for a quantitative analysis of the C-Pd films. In the case of thin films, the penetration depth of an electron beam can be greater than the film thickness and thus the elements originating from the substrate can be observed. When the films had a proper thickness, the quantitative analysis registered only the elements included in the films. For all films the concentration of Pd was determined as the function of the palladium and carbon content in the films. In this way the quantitative analysis of the Pd/C content ratio in C-Pd films was calculated. Table 2 presents the results of the AFM studies of the average surface roughness (Ra) and EDS analysis. Table 2 also shows the values of the film thickness (D) measured in a cross-section with SEM.

Table 2: Surface analysis.

	Average surface roughness	Pd content	D
	(Ra) [nm]	[wt. %]	[nm]
P1	4.65	9.86	503
P2	4.77	8.37	930
Р3	1.34	22.93	450

Depending on the parameters of the PVD processes, films with various thickness and Pd content were obtained. The films P1 and P2 have a similar average roughness and a similar Pd composition (Table 2). Both films contain less than 10 % palladium, but P1 is thinner than P2 (Figure 4a, b). The smoothest film, P3, contains the highest percentage by weight of palladium (22.93 wt. %). This sample is also the thinnest (Figure 4c). In our experiment we are using source boats that contain the same amount of Pd acetate material (54 mg) with time being the crucial factor. When time is to long (e.g. 10 minutes) all material from the boat is evaporated and ratio of evaporating fullerene is lower. Palladium acetate has a lower evaporation temperature than the fullerene and thus a situation can a rise whereby the palladium acetate may completely evaporate

within the first minutes and its vapour does not deposit on the substrate. This is the reason why wt % of Pd in sample P1 (10 minutes) is much lower than in sample P3 (8 minutes). Another important factor is the current through the source of the palladium acetate. For higher currents (P1,  $I_{Pd}$  = 1.2 A) evaporation may be too violent, for lower currents (P3,  $I_{Pd}$  = 1.1 A) evaporation of the source is calmer. It is also seen that distance is not as important a factor as the time is in this PVD experiment. The palladium content in samples P1 (d = 69 mm) and P2 (d = 54 mm) are similar, although the distances are different. The distance from the sources to the substrates affects the thickness of the C-Pd film. The differences in thickness for sample P1 and P2 is due to the probability of collision between  $C_{60}$  molecules on the way to the substrate. When D is small the probability of collision between  $C_{60}$  molecules is lower. When D is large there are many intermolecular collisions, some of which are deposited on to the casing wall where the substrate is placed. Different barrier layers of Si were used to separate the C-Pd films from the conductive substrate and to improve the adhesion of C-Pd film to the substrate. The C-Pd films containing palladium nanograins incorporated in a carbon matrix, investigated in this paper, seem to be promising materials for gas sensing applications. Hydrogen sensors with active C-Pd films operate on the principle of measuring the changes in the film resistance under the influence of hydrogen. It is also crucial that the active layer in this sensor has the best mechanical properties. The thickness of the DLC layer of sample P1 is 160 nm.  $SiO_2$  layers, 390 nm thick, separate the P2 and P3 films.

From our SEM studies we can see that the structure of C-Pd deposited on the DLC barrier layer is more uniform than C-Pd films of different thickness deposited on  $SiO_2$ . Images of the cross-section of samples P2 and P3 show visible grain structure. Films have better adhesion to  $SiO_2$  layer than to DLC. P1 film does not adhere to the substrate over the entire surface. Gaps between the C-Pd film and DLC layer are visible. In addition, it seems that homogeneity and adhesion of films depends on the defects propagating from substrate trough interlayer. In case of sample P3, the substrate had less defects than the other samples.

#### 4 Nanoindentation results

The value of the indentation depth, where the first signs of delamination were observed, are 350 nm, 440 nm and 225 nm for samples P1, P2 and P3, respectively. Changes in the hardness and elasticity modulus below these values reflect the mechanical properties of the C-Pd film. Figure 5

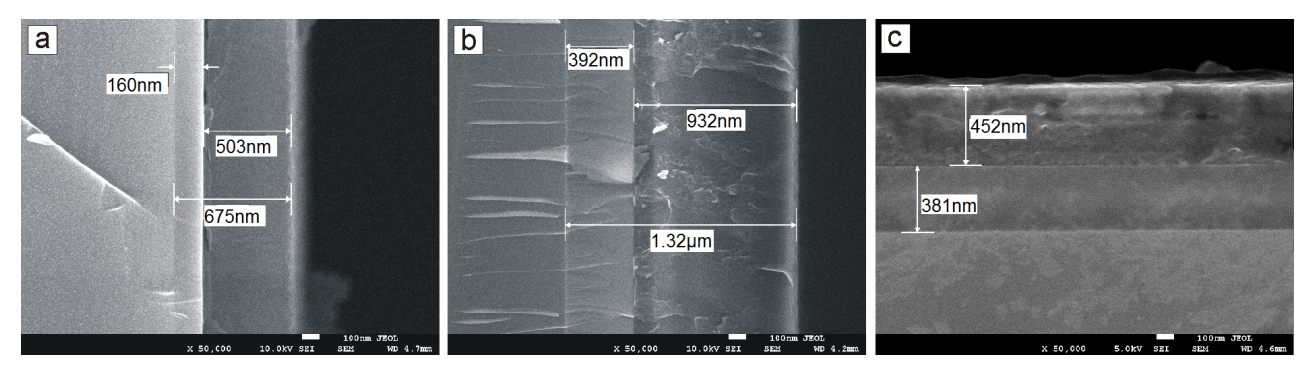


Figure 4: Cross-section obtained with SEM of a) P1; b) P2; c) P3.

shows an image of sample P3 with coating delamination formed during nanoindentation tests.

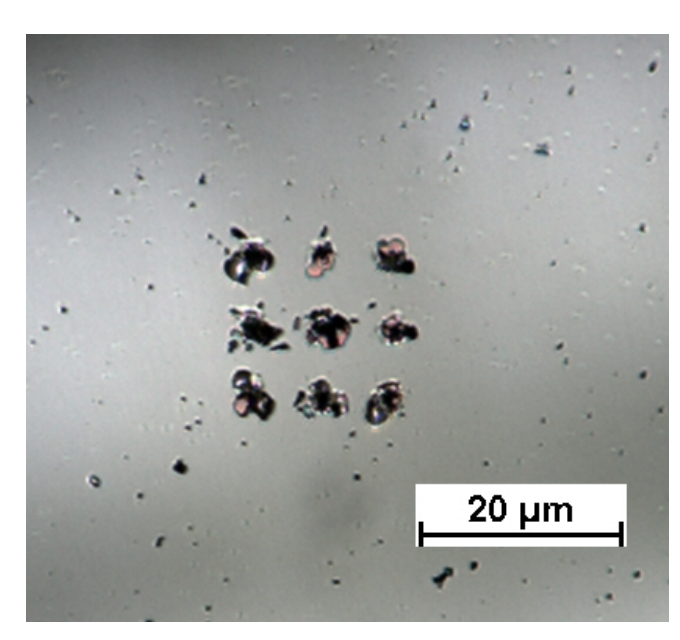


Figure 5: Image of P3 with cracks (delamination) - layers formed during nanoindentation test.

The hardness and elastic modulus as a function of indentation depth are shown in Figure 6 and Figure 7, respectively.

In all these films, it is observed that the surface is coated with a thin layer a few nanometers thick. The indenter tip penetrates into the sample after breaking of the superficial layer (A), which can be seen in Figure 6. The highest drop in hardness is observed for samples P1 and P2 (blue and red line, repectively) and the lowest for sample P3 (green line). The hardness of the superficial layer is about 0.2 GPa (P1 and P2) and 0.5 GPa (P3), depending on the type of the films. According to the rule of Bueckle the indentation depth should be 10 % or less of the total

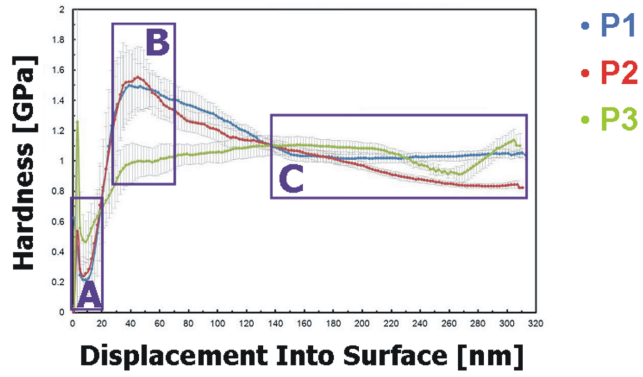


Figure 6: Hardness as a function of displacement into surface of different C-Pd films.

film thickness to avoid influencing the substrate. The next area in Figure 6, depicted as area (B), provides information about the mechanical properties of C-Pd films. For area B, samples P1 and P2 demonstrate a maximum hardness of 1.6 GPa (both with similar Pd concentration). P3 has lower hardness that amounts to 1 GPa. The area (C) in Figure 6 reflects the impact of buffer layers (DLC or  $SiO_2$ ) on the results. It can be noticed that the thinnest sample - P3 is characterised by the highest hardness, which is 1.1 GPa. It is confirmed that the results in area (C) are with influenced by the substrate. The hardness in area (C) of P2 is 1 GPa and P1 is 0.8 GPa. Different technological parameters can cause differences in the distribution of the Pd precursor in the prepared C-Pd films in the form of the carbonaceous matrix. The study on these effects can be found in our papers [13, 14]. The parameters of the technological PVD process have a strong influence on the topography, structure and morphology of carbon films containing Pd nanograins (C-Pd films). It was observed that the films contain different sizes of fcc nanocrystals, embedded in a carbon matrix. Our previous studies have shown that the matrix could be composed of many forms of carbon (fullerite grains, amorphous carbon grains, loosely connected graphite planes or 76 — J. Rymarczyk et al. DE GRUYTER OPEN

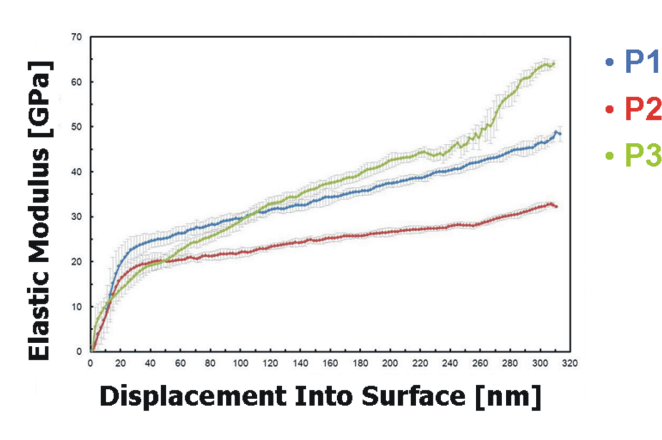


Figure 7: Elastic modulus as a function of displacement into surface of different C-Pd films.

even graphite nanograins). The matrix form and grain size depend on the PVD process conditions. C-Pd film mechanical properties depend on the form of this carbonaceous matrix. Comparisons of the mechanical properties of these C-Pd films with pure  $C_{60}$ , diamond or graphite films as well as to pure palladium film [11, 16] show that these properties are completely different.

Figure 7 presents the elastic modulus versus penetration depth of C-Pd films. The elastic modulus depth profiles of samples P1 and P2 demonstrate a clear inflection point at a depth of  $\sim$ 20 nm. This result confirms that C-Pd films are covered by a thin superficial layer with different mechanical properties when compared with the interior. The inflection point for P3 occurs earlier (on the 5 nm of displacement into surface) than for other samples. This sample is the thinnest, which may suggest that its superficial layer is also the thinnest. P1 has the highest elastic modulus (24 GPa (blue line)) which is less than 10 % of the total film thickness. P3 has the lowest elastic modulus (7 GPa (green line)). The elastic modulus of P2 (red line) is 18 GPa.

In order to determine the adhesion of C-Pd films to the substrate, a nanoscratch test was used. The results presented in Figure 8 show the three typical critical failure points observed for C-Pd films.

The normal force during the scratch test increased linearly from 0 mN to 20 mN along a scratch length of 100  $\mu m$ . The scratch velocity was 1  $\mu m/s$ . Critical load to full delamination of the film was calculated according to the friction coefficient changes during the test, penetration depth registration and optical microscopy analysis of the scratch track. The composition of the material as well as the thickness affects the properties of thin films [15]. The results of nanoscratch studies for different C-Pd films are summarised in Table 3.

Table 3: Surface analysis.

2	Critical load	Standard	Penetration Depth
R	[mN]	deviation [mN]	At Critical Load [nm]
P1	2.31	0.24	348
P2	4.18	0.55	440
Р3	1.66	0.34	251

The highest value of critical load to delamination was measured for P2 (4.18 mN), which has the greatest thickness. The value of the penetration depth for which the first signs of delamination was observed is 440 nm for this C-Pd film. The film thickness measured with a post-scratch test analysis is similar to the values obtained from the cross-section analysis in SEM studies for all samples. The critical force of P3 is 1.66 mN. Its thickness is close to the P1 thickness. The differences in the penetration depth at critical load may be caused by differences in the Pd contents and adhesion to a different interlayer (DLC and  $SiO_2$ ). The critical load at which the coating detaches from the substrate in the case of sample P1 is 2.31 mN. Penetration depth at critical load for sample P1 is 348 nm and for sample P3 it is 251 nm.

#### 5 Conclusion

Mechanical properties of carbon films containing Pd nanograins (C-Pd films) are substantially influenced by their microstructure, morphology and palladium content. It has been recognised that the parameters of the technological process have a strong influence on the topography and thickness of these films. The film containing the highest percentage of palladium in relation to carbon has the smoothest surface. It has been shown that both the current intensity through sources ( $I_{C60}$ ,  $I_{Pd}$ ) and sources-substrate distance in the PVD process affect the thickness of the C-Pd films. The results of the cross-section analysis in SEM studies and a scratch test are consistent and confirm the differences in the thickness of C-Pd films. It was also noticed that the duration of the PVD process has an impact on the contents of palladium in C-Pd films. With a lower current intensity through palladium acetate and shorter duration of the PVD process a film with higher palladium content was obtained. The examination of nanoindentation revealed the existence of a thin superficial layer on the surface of C-Pd films characterised by distinct mechanical properties. The C-Pd film containing the highest percentage of palladium has the lowest hardness. This film also demonstrated

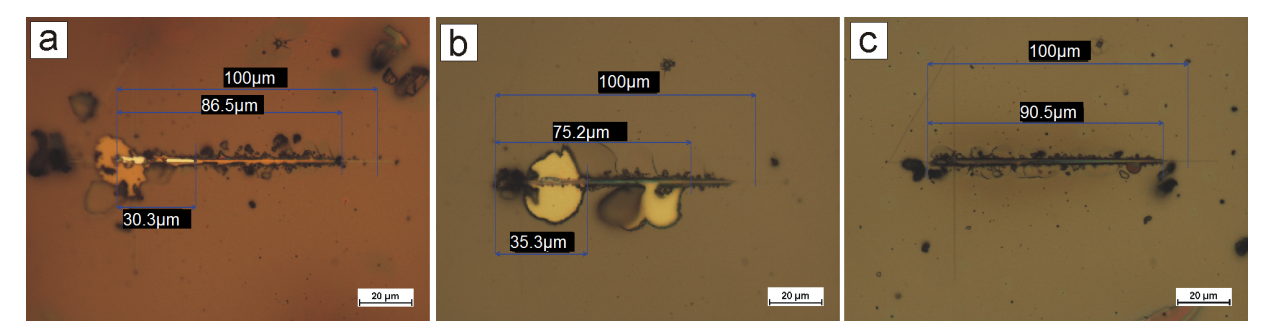


Figure 8: Images of the scratch at a) P1; b) P2; c) P3.

the lowest modulus of elasticity. Films P1 and P2 with similar palladium contents but different thickness have similar hardness but the modulus of elasticity of P1 is the higher. It is also seen that the thickness of C-Pd films are not as important a factor as the content of palladium is in the differences in the morphology of the carbonaceous matrix. Effects of intermediate layers on nanoindentation test results is difficult to interpret because C-Pd films have different thickness and morphology.

**Acknowledgement:** The authors would like to thank Dr Miroslaw Kozlowski for the SEM study of our samples. This research was co-financed by the European Regional Development Fund within the Innovative Economy Operational Programme 2007-2013 (title of the project "Development of technology for a new generation of the hydrogen and hydrogen compounds sensor for applications in above normative conditions", No. UDA-POIG.01.03.01-14-071/08-11).

#### References

[1] B.N. Kuznetsov et al., React. Kinet. Catal. L. 83, 361 (2004)

- [2] V.C. Diculescu, A.-M. Chiorcea-Paquim, O. Corduneanu, A.M. Oliveira-Brett, J. Solid State Electr. 11, 887 (2007)
- [3] D.S. Dos Santos, P.E.V. De Miranda, J. Mater. Sci. 32, 6311 (1997)
- [4] M. Ohno, N. Okamura, T. Kose, T. Asada, K. Kawata, J. Porous Mat. 19, 1063 (2012)
- [5] Min G. Chung et al., Sensor Actuat. B-Chem. 169, 387 (2012)
- [6] Lu Wang et al., ACS Nano 3, 2995 (2009)
- [7] Jung-Eun Lee, Hyun-Joon Kim, Dae-Eun Kim, J. Mech. Sci. Technol. 24, 97 (2010)
- [8] G. Timp, Nanotechnology (Springer-Verlag, New York, 1999)
- [9] A.C. Fischer-Cripps, Nanoindentation (Springer-Verlag, New York, 2002)
- [10] E. Czerwosz et al., Vacuum 82, 372 (2008)
- [11] J. Rymarczyk, E. Czerwosz, A. Richter, Cent. Eur. J. Phys. 9, 300 (2011)
- [12] Xiaodong Li, Bharat Bhushan, Mater. Charact. 48, 11 (2002)
- [13] E. Czerwosz, P. Dluzewski, E. Kowalska, M. Kozlowski, J. Rymarczyk, Phys. Status Solidi C 7-8, 2527 (2011)
- [14] J. Rymarczyk, A. Kaminska, J. Keczkowska, M. Kozlowski, E. Cz-erwosz, Opt. Appl., XLIII, 123 (2013)
- [15] T.R. Hull, J.S. Colligon, A.E. Hill, Vacuum 37, 327 (1987)
- [16] A. Richter, R. Ries, R. Smith, M. Henkel, B. Wolf, Diam. Relat. Mater. 9, 170 (2000)